RSC Medicinal Chemistry

ROYAL SOCIETY OF CHEMISTRY

RESEARCH ARTICLE

Cite this: *RSC Med. Chem.*, 2023, **14**, 2100

Design, synthesis, and biological evaluation of 3,3′-diindolylmethane *N*-linked glycoconjugate as a leishmanial topoisomerase IB inhibitor with reduced cytotoxicity†

Parampreet Kour, [a] Pallavi Saha, ‡[b] Srija Bhattacharya, ‡[c] Diksha Kumari, [ad] Abhipsa Debnath,[e] Amit Roy,[e] Deepak K. Sharma, [b] Debaraj Mukherjee *[df] and Kuljit Singh *[ad]

Leishmaniasis, one of the neglected diseases, ranks second to malaria in the cause of parasitic mortality and morbidity. The present chemotherapeutic regimen faces the limitations of drug resistance and toxicity concerns, raising a great need to develop new chemotherapeutic leads that are orally administrable, potent, non-toxic, and cost-effective. Several research groups came forward to fill this therapeutic gap with new classes of active compounds against leishmaniasis, one such being 3,3′-diindolylmethane (DIM) derivatives. We tried to link this concept with another promising approach of glycoconjugation to study how glycosylated groups work differently from non-glycosylated ones. In the present study, a series of 3,3′-DIM derivatives have been synthesized and screened for their anti-leishmanial potency on *Leishmania donovani* promastigotes. Next, we synthesized the β-*N*,*N*′ glycoside of potent compound **3d** using indole–indoline conversion, Fischer-type glycosylation, 2,3-dichloro-5,6-dicyano-1,4-benzoquionone (DDQ) oxidation, and molecular iodine catalyzed coupling with a suitable aldehyde in reasonable overall yield. The biological evaluation revealed that glycosides had reduced cytotoxic effects on the J774A.1 macrophage cell line. The enzyme inhibition study confirms that the glycoside derivatives have significant inhibitory activity against the leishmanial topoisomerase IB enzyme. Molecular docking further displayed the better binding efficiency of glycoside **13** with the target enzyme, suggesting the involvement of more H-bond interactions in the case of glycosides as compared to free drugs. Therefore, this work helps in proposing the fact that the addition of sugar moieties adds some favorable characteristics to free inhibitors, making it a promising approach for future clinical diagnostic and therapeutic applications, which can prove to be a valuable arsenal in combating such neglected diseases.

Received 10th May 2023,
Accepted 25th August 2023

DOI: 10.1039/d3md00214d

rsc.li/medchem

1. Introduction

Leishmaniasis, a neglected parasitic disease, affects millions of people worldwide, posing a serious health threat in developing countries. The causative agent of the disease is a unicellular protozoan parasite belonging to the genus *Leishmania* (order *Kinetoplastida* and family Trypanosomatidae).[1,2] The protists exhibit a digenetic life cycle appearing in two different forms. The flagellated promastigote form of the parasite resides extracellularly in the sand-fly gut, whereas the non-flagellated amastigote form is found in the host macrophages.[3,4] First-line drugs for the treatment of leishmaniasis include pentavalent antimonials, followed by amphotericin B, miltefosine, and paromomycin as second-line drugs of choice. These medications have numerous limitations, including variable efficacy and toxic side effects.[5,6] For these reasons, developing new anti-leishmanial compounds with novel molecular targets and intervention strategies with improved drug therapy remains desirable.

Amongst various anti-leishmanial scaffolds reported, bisindoles or diindolylmethanes showed promising

[a] *Infectious Diseases Division, CSIR – Indian Institute of Integrative Medicine, Canal Road, Jammu, 180001, India. E-mail: singh.kuljit@iiim.res.in; Tel: +91 191 2585006 13 Ext: 333*
[b] *Department of Pharmaceutical Engineering and Technology, Indian Institute of Technology Banaras Hindu University, Varanasi-221005, India*
[c] *Natural Products & Medicinal Chemistry Division, CSIR – Indian Institute of Integrative Medicine, Jammu, 180001, India. E-mail: debaraj@jcbose.ac.in*
[d] *Academy of Scientific and Innovative Research (AcSIR), Ghaziabad-201002, India*
[e] *Department of Biotechnology, Savitribai Phule Pune University, Pune-411007, India*
[f] *Department of Chemical Sciences, Unified Academic Campus, Bose Institute, Kolkata, 700091, India*

† Electronic supplementary information (ESI) available. See DOI: **https://doi.org/10.1039/d3md00214d**

‡ These authors equally contributed to this work.

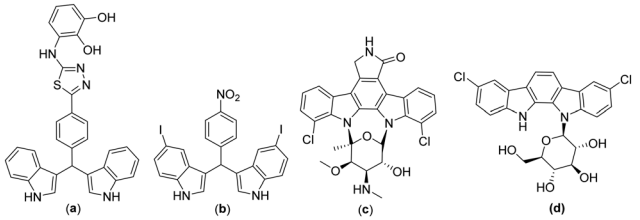

Fig. 1 Literature reported 3,3′-DIM active against the *Leishmania* parasite (a and b) and natural products based on *N*-glycosylated indole-containing compounds staurosporine (c) and tjipanazole (d).

pharmacological activity against the *Leishmania* parasite (Fig. 1a).[7] It has been observed that dimeric indole alkaloids proved to be better anti-bacterial and anti-leishmanial agents when compared to monomeric indole alkaloids (Fig. 1b).[8] 3,3′-Diindolymethane (DIM) is a major acid condensation product of indole-3-carbinol, a natural compound found in cruciferous vegetables of the genus *Brassica*.[9] It is a novel immuno-modulator that induces G1 cell cycle arrest in breast cancer cells by up-regulation of p21 leading to apoptotic signaling. Roy's group[10] reported 3,3′-DIM as a potent topoisomerase I poison that directly stabilizes the formation of topoisomerase I–DNA cleavable complexes in leishmanial cells. 3,3′-DIM acts as a non-competitive inhibitor of the topoisomerase I interface, trapping the cleavable complexes by preventing the religation step. It has also been reported to inhibit the mitochondrial H^+-ATP synthase leading to programmed cell death in *Leishmania* parasites. Due to the diverse pharmacological activities of these diindolylmethanes and their unprecedented role in biological chemistry, plenty of synthetic methods with the development of new catalytic processes for the generation of 3,3′-DIM analogues are always welcomed in organic chemistry.

With recent advancements in glycobiology and glycochemistry, glycosides are crucial in modifying new therapeutics and have significantly contributed to drug discovery.[11] This concept of glycoconjugation has been widely used in natural product chemistry to improve non-glycosylated therapeutics, including colchicine, mitomycin, podophyllotoxin, various anti-cancer drugs such as taxol, rapamycin, methotrexate, and doxorubicin, anti-viral drugs like azidothymidine and stavudine, and some anti-tubercular drugs, for example, rifampicin.[12–14] The above modifications show that the sugar residue attached to the indolocarbazole ring system plays a vital role in both DNA binding and topoisomerase I inhibition.[15] Further, it is well documented that glycosylation enhances the pharmacological and pharmacokinetic properties of designed molecules to determine their specificity at the tissue, cellular or molecular levels.[16] Glycosylated macromolecular carriers impart some gratifying characteristics in drug molecules, making them a vital candidate in medicinal chemistry. These carriers have numerous path-breaking advantages in altering the pharmacokinetic profile of drugs, drug stability with sustained and controlled release, multifaceted drug delivery vehicles, enhancement in biostability, bioadhesive properties, solubility, and reduction in toxicity associated with unmodified therapeutic agents.[17,18]

Specific effects of glycosylation on the improvement of conventional therapeutics include site-specific targeting, efficient protein–protein binding, protein molecular stability, and effective protein structural, conformational, and torsional changes.[19] Addition of glycans has led to the sustained release of drugs with an overwhelming increase in bioadhesive properties of free drugs, making it a promising approach to be explored for oral immunization and vaccine delivery systems. Glycosylation of digitoxin by Langenhan's group[20] and digoxin by Wang's group[21] resulted in reduced cytotoxic effects of the drug on human cancer cell lines. Griffith's group[22] made modifications to vancomycin by glycosylating it with *N*-substituted glucopyranose. The synthesized glycoside was found to be 40 times more effective against various vancomycin-resistant strains than conventional vancomycin. The involvement of carbohydrates in intercellular recognition and various biological processes has paved the way for its utilization as a natural route for developing new therapeutic carriers. Among different glycoside classes (O/N/C/S), categorized based on glycosidic linkage to anomeric carbon, *N*-glycosides are known to be metabolically more stable with an additional degree of stability towards enzymatic hydrolysis. In contrast, *O*-glycosides, though common in nature, are susceptible to rapid hydrolysis. Also, there are natural products like staurosporine and tjipanazole E (Fig. 1c and d) in which a single sugar component is attached to one or both indoles of an indolocarbazole moiety. Because of their great potential, *N*-glycosidic forms are considered privileged scaffolds to be worked upon. The ideology has encouraged us to glycosylate bioactive analogues of 3,3′-DIM for developing promising anti-leishmanial lead compounds.

In the present study, we have synthesized a series of 3,3′-DIM derivatives by multiple substitutions between indoles and aldehydes, followed by glycosylation of a potent 3,3′-DIM analog. Also, we have observed that fluoro analogs exhibit strong inhibitory effects on leishmanial parasite growth and may be useful anti-leishmanial scaffolds to be investigated in the near future for the development of sensible chemotherapeutic strategies to treat leishmaniasis and address the issue of protracted drug resistance. Furthermore, computational predictions and enzyme inhibition assays displayed better binding affinity of glycosylated derivatives with the target protein compared to the non-glycosylated ones, and their reduced cytotoxicity related to the fact that this concept of glycoconjugation should be explored more to improve the conventional therapeutics in terms of safety, efficacy, stability, and toxicity.

2. Materials and methods

2.1. Experimental section

2.1.1. General. All the chemicals used were purchased from Sigma-Aldrich, SRL, and TCI with 98% purity and were

used as received without any need for further purification. The compounds synthesized were characterized using ^{1}H NMR spectra recorded on a Bruker Avance DPX FT-NMR 400 MHz instrument (^{1}H) at 400 MHz and (^{13}C) at 100 MHz, respectively. ^{19}F NMR spectra were recorded at 376 MHz. Column chromatography using silica gel, Merck grade 60–120 mesh size, and hexane–ethyl acetate (EtOAc) and dichloromethane (DCM)–methanol (MeOH) as eluents was performed to obtain the purified product, followed by performing thin-layer chromatography (TLC) on 0.25 mm E. Merck pre-coated silica gel plates (60 F254).

2.1.2. General procedure for the synthesis of substituted 3,3′-DIM compounds 2a–5d. A mixture of benzaldehydes (1 mmol), indoles (2 mmol), and montmorillonite K-10 clay (307 mg) in DCM (15 ml) was stirred at room temperature for 5–10 hours. The progress of the reaction was monitored by TLC. On completion of the reaction, the crude product was obtained by filtering the reaction mixture and concentrating the filtrate on a vacuo-rotavapor. The crude filtrate was purified by column chromatography (ethyl acetate : hexane) to afford the pure DIM compound.

2.1.3. Procedure followed for the synthesis of glycoside DIM derivative 12 from 6

2.1.3.1. Procedure for the preparation of compound 7. A solution of 5-bromoindole (3.2 mmol) in acetic acid was stirred for 10 min at 12 °C, and sodium cyanoborohydride (12 mmol) was added portion-wise under a nitrogen atmosphere at the same temperature. The reaction mixture was stirred for 2 h and monitored by TLC. After completion of the reaction, the mixture was neutralized with 50% sodium hydroxide (10 ml). Finally, EtOAc was added, and the mixture was stirred for 30 min. The EtOAc layer was separated, the extraction was repeated two more times, and the combined EtOAc layers were washed with brine. After removing the organic solvent, a viscous oil was obtained which was purified on a silica gel column.

*2.1.3.2. Procedure for the synthesis of compound **8**.* D-Glucose (3.05 mmol) was added to a solution of **7** (6.1 mmol) in a mixture of ethanol (46.7 ml) and water (3.1 ml). The mixture was heated to 90 °C for 24 h. After concentration under vacuum, the resulting mixture was purified by flash chromatography (eluent EtOAc–MeOH from 98 : 2 to 90 : 10) to give the corresponding glycosyl-indoline **8**.

*2.1.3.3. Procedure for the synthesis of compound **9**.* A solution of **8** (3.55 mmol) in pyridine (10.7 ml) was cooled to 0 °C before the addition of acetic anhydride (7.9 ml). The reaction mixture was stirred at room temperature for 24 h. After the addition of water and extraction with EtOAc, the organic phases were washed with saturated aqueous sodium bicarbonate ($NaHCO_3$) and water until neutral. After drying over magnesium sulfate ($MgSO_4$), the solvent was removed, and the residue was purified by flash chromatography (eluent cyclohexane–EtOAc from 80 : 20 to 40 : 60) to give the corresponding protected compounds.

*2.1.3.4. Procedure for the synthesis of compound **10**.* 2,3-Dichloro-5,6-dicyano-1,4-benzoquionone (DDQ) (0.4 mmol) was added to a solution of **9** (0.36 mmol) in 1,4-dioxane (16 ml). The mixture was stirred at room temperature for 24 h and hydrolyzed with saturated aqueous $NaHCO_3$. The solid residue obtained was concentrated, and EtOAc was added. The added EtOAc was removed by filtration. The filtrate was dried over $MgSO_4$ and concentrated under vacuum to give a residue, which was purified by flash chromatography (eluent EtOAc–MeOH from 100 : 0 to 90 : 10) to give the corresponding glycosyl-indole.

*2.1.3.5. Procedure for the synthesis of compound **11**.* Sodium methoxide in MeOH (1.0 M freshly prepared solution) was added to compound **10** (2.5 mmol) in MeOH (25 ml), which was precooled on an ice bath. The reaction mixture was stirred for 30 minutes, and the temperature was raised from 0 °C to room temperature. The solvent was evaporated under reduced pressure; the residue was dissolved in water and acidified to pH 6 by the addition of Amberlite-H^+ resin. The resin was removed by filtration, and the filtrate was freeze-dried to give the deacetylated product **11**.

*2.1.3.6. Procedure for the synthesis of compound **12**.* A mixture of 4-fluorobenzaldehyde (1 mmol), compound **10** (2 mmol), and I_2 (0.2 mmol) in acetonitrile (10 ml) was stirred at room temperature for a few seconds. After completion of the reaction (TLC, <1 min), the mixture was treated with aqueous sodium thiosulfate ($Na_2S_2O_3$) solution (5%, 10 ml), and the product was extracted with EtOAc (3 × 15 ml). The combined organic layer was dried with anhydrous sodium sulfate, concentrated *in vacuo*, and purified by column chromatography (ethyl acetate : petroleum ether = 4 : 6) to afford the pure product.

*2.1.3.7. Procedure for the synthesis of compound **13**.* Sodium methoxide in MeOH (1.0 M freshly prepared solution) was added to compound **12** (2.5 mmol) in MeOH (20 ml), which was precooled on an ice bath. The reaction mixture was stirred for 30 min, during which the temperature rose from 0 °C to room temperature. The solvent was evaporated under reduced pressure; the residue was dissolved in water and acidified to pH 6 by the addition of Amberlite-H^+ resin. The resin was removed by filtration, and the filtrate was freeze-dried to give the deacetylated product **13**. The product **13** was further crystallized in methanol.

2.1.4. Spectral data of synthesized compounds

*2.1.4.1. 3,3′-((4-Nitrophenyl)methylene)bis(1H-indole) (**2a**).* Yellow amorphous solid (129 mg, 83% yield); Mp 219–220 °C; ^{1}H NMR (400 MHz, DMSO) δ 10.95 (s, 2H), 8.16 (s, 2H), 7.62 (s, 2H), 7.33 (d, J = 29.4 Hz, 4H), 7.06 (s, 2H), 6.90 (s, 4H), 6.04 (s, 1H).

*2.1.4.2. 3,3′-((4-Bromophenyl)methylene)bis(1H-indole) (**2b**).* Brown amorphous solid (143 mg, 85% yield); Mp 100–102 °C; ^{1}H NMR (400 MHz, $CDCl_3$) δ 7.88 (s, 2H), 7.40–7.35 (m, 3H), 7.35–7.31 (m, 3H), 7.21–7.15 (m, 4H), 7.01 (ddd, J = 7.9, 7.1, 0.9 Hz, 2H), 6.61 (dd, J = 2.3, 0.9 Hz, 2H), 5.83 (s, 1H). ^{13}C NMR (100 MHz, $CDCl_3$) δ 143.1, 136.7, 131.3, 130.5, 126.9, 123.6, 122.1, 119.9, 119.8, 119.4, 119.1, 111.1, 39.7. HRMS (ESI): calculated for $C_{23}H_{18}BrN_2$ $[M + H]^+$ 401.0609, found 401.0653.

*2.1.4.3. 3,3′-((4-Chlorophenyl)methylene)bis(1H-indole) (**2c**).* Brownish red amorphous solid (97 mg, 64% yield); Mp 104–106 °C; ^{1}H NMR (400 MHz, $CDCl_3$) δ 7.88 (s, 2H), 7.34 (t, J = 7.6 Hz, 4H), 7.25–7.21 (m, 4H), 7.19–7.14 (m, 2H), 7.06–6.96 (m, 2H), 6.60 (s, 2H), 5.84 (s, 1H). ^{13}C NMR (100 MHz, $CDCl_3$) δ 142.6, 136.7, 131.8, 130.1, 128.4, 126.9, 123.6, 122.1, 119.8, 119.4, 119.2, 111.1, 39.6. HRMS (ESI): calculated for $C_{23}H_{17}N_2Cl$ $[M + H]^+$ 357.1114, found 357.1159.

*2.1.4.4. 3,3′-((4-Fluorophenyl)methylene)bis(1H-indole) (**2d**).* Dark brown amorphous solid (110 mg, 76% yield); Mp 108–110 °C; ^{1}H NMR (400 MHz, $CDCl_3$) δ 7.83 (s, 2H), 7.34 (dd, J = 11.5, 8.1 Hz, 4H), 7.29–7.25 (m, 2H), 7.17 (t, J = 7.6 Hz, 2H), 7.00 (t, J = 7.5 Hz, 2H), 6.96–6.89 (m, 2H), 6.63–6.57 (m, 2H), 5.85 (s, 1H). ^{13}C NMR (100 MHz, $CDCl_3$) δ 161.4 (d, J^1 = 243.5 Hz), 139.7 (d, J^4 = 3.0 Hz), 136.7, 130.1 (d, J^3 = 7.8 Hz), 126.9, 123.6, 122.1, 119.9, 119.6, 114.9 (d, J^2 = 21.2 Hz), 111.1, 39.5. ^{19}F NMR (377 MHz, $CDCl_3$) δ −117.3. HRMS (ESI): calculated for $C_{23}H_{17}FN_2$ $[M + H]^+$ 341.1409, found 341.1454.

*2.1.4.5. 3,3′-(p-Tolylmethylene)bis(1H-indole) (**2e**).* Orange amorphous solid (111 mg, 78% yield); Mp 96–97 °C; ^{1}H NMR (400 MHz, $CDCl_3$) δ 7.81 (s, 2H), 7.38 (d, J = 7.8 Hz, 2H), 7.31 (d, J = 8.1 Hz, 2H), 7.21 (d, J = 8.0 Hz, 2H), 7.18–7.11 (m, 2H), 7.07 (d, J = 7.8 Hz, 2H), 6.99 (td, J = 7.1, 3.5 Hz, 2H), 6.61 (dd, J = 2.2, 0.7 Hz, 2H), 5.83 (s, 1H), 2.31 (s, 3H). ^{13}C NMR (100 MHz, $CDCl_3$) δ 141.0, 136.7, 135.5, 128.9, 128.6, 127.1, 123.6, 121.9, 119.9, 119.9, 119.2, 111.0, 39.8, 21.1. HRMS (ESI): calculated for $C_{24}H_{21}N_2$ $[M + H]^+$ 338.1694, found 338.1705.

*2.1.4.6. 3,3′-((4-Methoxyphenyl)methylene)bis(1H-indole) (**2f**).* Reddish brown amorphous solid (96 mg, 64% yield); Mp 187–189 °C; ^{1}H NMR (400 MHz, $CDCl_3$) δ 7.88 (s, 2H), 7.38 (d, J = 8.0 Hz, 2H), 7.33 (d, J = 8.1 Hz, 2H), 7.24 (s, 1H), 7.22 (s, 1H), 7.15 (ddd, J = 8.1, 7.1, 1.1 Hz, 2H), 6.99 (ddd, J = 8.0, 7.1, 1.0 Hz, 2H), 6.85–6.70 (m, 2H), 6.70–6.59 (m, 2H), 5.82 (s, 1H), 3.76 (s, 3H). ^{13}C NMR (100 MHz, $CDCl_3$) δ 157.9, 136.7, 136.2, 129.6, 127.1, 123.6, 121.9, 120.0, 119.9, 119.2, 113.6, 111.0, 55.2, 39.3. HRMS (ESI): calculated for $C_{24}H_{20}N_2O$ $[M + H]^+$ 353.1578, found 353.1576.

*2.1.4.7. 3,3′-((4-(Methylthio)phenyl)methylene)bis(1H-indole) (**2g**).* Orangish brown amorphous solid (112 mg, 72% yield); Mp 108–110 °C; ^{1}H NMR (400 MHz, $CDCl_3$) δ 7.84 (s, 2H), 7.37 (d, J = 7.9 Hz, 1H), 7.33 (d, J = 8.1 Hz, 2H), 7.25 (d, J = 1.6 Hz, 1H), 7.24 (s, 1H), 7.16 (dt, J = 7.2, 3.3 Hz, 4H), 7.00 (dd, J = 7.9, 7.1 Hz, 2H), 6.61 (s, 2H), 5.83 (s, 1H), 2.44 (s, 3H). ^{13}C NMR (100 MHz, $CDCl_3$) δ 141.2, 136.7, 135.5, 129.3, 127.0, 126.7, 123.6, 122.0, 119.9, 119.5, 119.3, 111.1, 39.7, 16.0. HRMS (ESI): calculated for $C_{24}H_{20}N_2S$ $[M + H]^+$ 369.1414, found 369.1425.

*2.1.4.8. 3,3′-((4-Nitrophenyl)methylene)bis(5-bromo-1H-indole) (**3a**).* Straw yellow amorphous solid (105 mg, 79% yield); Mp 189–190 °C; ^{1}H NMR (400 MHz, $CDCl_3$) δ 8.20–8.10 (m, 4H), 7.43 (dd, J = 5.7, 4.9 Hz, 4H), 7.30–7.26 (m, 4H), 6.65 (dd, J = 2.4, 0.8 Hz, 2H), 5.85 (s, 1H). ^{13}C NMR (100 MHz, $CDCl_3$) δ 150.8, 146.7, 135.3, 129.4, 128.2, 125.4, 124.8, 123.8, 121.9, 117.4, 113.0, 112.8, 39.8.

*2.1.4.9. 3,3′-((4-Bromophenyl)methylene)bis(5-bromo-1H-indole) (**3b**).* Brown semi-solid (120 mg, 85% yield); ^{1}H NMR (400 MHz, $CDCl_3$) δ 8.02 (s, 2H), 7.43 (dd, J = 14.0, 4.6 Hz, 4H), 7.25 (dd, J = 3.9, 1.1 Hz, 4H), 7.16 (s, 2H), 6.75–6.53 (m, 2H), 5.71 (s, 1H). ^{13}C NMR (100 MHz, $CDCl_3$) δ 142.1, 135.3, 131.5, 130.3, 128.4, 125.1, 124.7, 122.1, 120.3, 118.4, 112.8, 112.7, 39.3. HRMS (ESI): calculated for $C_{23}H_{16}N_2Br_3$ 556.8819, found 556.8864.

*2.1.4.10. 3,3′-((4-Chlorophenyl)methylene)bis(5-bromo-1H-indole) (**3c**).* Maroon semi-solid (106 mg, 81% yield); ^{1}H NMR (400 MHz, $CDCl_3$) δ 8.01 (s, 2H), 7.45 (d, J = 0.7 Hz, 2H), 7.26–7.19 (m, 8H), 6.62 (d, J = 1.4 Hz, 2H), 5.72 (s, 1H). ^{13}C NMR (100 MHz, $CDCl_3$) δ 141.6, 135.3, 132.2, 129.9, 128.6, 128.4, 125.1, 124.7, 122.1, 118.5, 112.8, 112.6, 39.3. HRMS (ESI): calculated for $C_{23}H_{16}N_2ClBr_2$ $[M + 1]^+$ 512.9324, found 512.9369.

*2.1.4.11. 3,3′-((4-Fluorophenyl)methylene)bis(5-bromo-1H-indole) (**3d**).* Red semi-solid (91 mg, 72% yield); ^{1}H NMR (400 MHz, $CDCl_3$) δ 8.00 (s, 2H), 7.45 (s, 2H), 7.25–7.21 (m, 6H), 6.97 (t, J = 8.6 Hz, 2H), 6.61 (s, 2H), 5.72 (s, 1H). ^{13}C NMR (100 MHz, $CDCl_3$) δ 161.5 (d, J^1 = 244.6 Hz), 138.7 (d, J^4 = 3.0 Hz), 135.3, 129.9 (d, J^3 = 7.9 Hz), 128.5, 125.1, 124.7, 122.2, 118.9, 115.2 (d, J^2 = 21.3 Hz). 112.7, 112.6, 39.1. ^{19}F NMR (377 MHz, $CDCl_3$) δ −116.65. HRMS (ESI): calculated for $C_{23}H_{16}N_2Br_2F$ $[M + H]^+$ 496.9620, found 496.9664.

*2.1.4.12. 3,3′-(p-Tolylmethylene)bis(5-bromo-1H-indole) (**3e**).* Copper brown semi-solid (101 mg, 81% yield); ^{1}H NMR (400 MHz, $CDCl_3$) δ 7.98 (s, 2H), 7.47 (d, J = 1.4 Hz, 2H), 7.26–7.22 (m, 3H), 7.19–7.13 (m, 3H), 7.09 (d, J = 8.0 Hz, 2H), 6.63 (s, 2H), 5.70 (s, 1H), 2.33 (s, 3H). ^{13}C NMR (100 MHz, $CDCl_3$) δ 140.0, 135.9, 135.3, 129.1, 128.6, 128.3, 124.9, 124.7, 122.3, 119.2, 112.6, 112.5, 39.4, 21.0. HRMS (ESI): calculated for $C_{24}H_{19}Br_2N_2$ $[M + H]^+$ 592.9870, found 592.9915.

*2.1.4.13. 3,3′-((4-Methoxyphenyl)methylene)bis(5-bromo-1H-indole) (**3f**).* Brown semi-solid (110 mg, 85% yield); ^{1}H NMR (400 MHz, $CDCl_3$) δ 8.07 (s, 2H), 7.47 (d, J = 0.6 Hz, 2H), 7.24–7.17 (m, 6H), 6.83 (d, J = 8.7 Hz, 2H), 6.63 (dd, J = 2.3, 0.8 Hz, 2H), 5.69 (s, 1H), 3.79 (s, 1H). ^{13}C NMR (100 MHz, $CDCl_3$) δ 158.1, 135.3, 135.2, 129.4, 128.6, 124.9, 124.7, 122.3, 119.3, 113.8, 112.6, 112.5, 55.2, 39.0. HRMS (ESI): calculated for $C_{24}H_{18}Br_2N_2O$ $[M + H]^+$ 508.9819, found 508.9864.

*2.1.4.14. 3,3′-((4-Methylthio)phenyl)methylene)bis(5-bromo-1H-indole) (**3g**).* Red semi-solid (101 mg, 76% yield); ^{1}H NMR (400 MHz, $CDCl_3$) δ 8.00 (s, 2H), 7.63–7.41 (m, 2H), 7.25–7.24 (m, 4H), 7.19 (s, 4H), 6.64 (dd, J = 2.4, 0.9 Hz, 2H), 5.71 (s, 1H), 2.47 (s, 3H). ^{13}C NMR (100 MHz, $CDCl_3$) δ 140.1, 136.1, 135.3, 129.0, 128.5, 126.7, 125.0, 124.7, 122.2, 118.9, 112.7, 112.6, 39.3, 15.9. HRMS (ESI): calculated for $C_{24}H_{18}Br_2N_2S$ $[M + H]^+$ 524.9599, found 524.9636.

*2.1.4.15. 3,3′-((4-Chlorophenyl)methylene)bis(5-fluoro-1H-indole) (**4a**).* Orange semi-solid (104.51 mg, 72% yield); ^{1}H NMR (400 MHz, $CDCl_3$) δ 7.98 (s, 2H), 7.25 (dd, J = 4.5, 2.7 Hz, 6H), 7.03–6.84 (m, 4H), 6.69 (d, J = 2.0 Hz, 2H), 5.70 (s, 1H). ^{13}C NMR (100 MHz, $CDCl_3$) δ 157.5 (d, J = 234.6 Hz), 141.8, 132.6 (d, J = 108.9 Hz), 129.9, 128.5, 127.1 (d, J = 9.7 Hz), 125.2, 118.9 (d, J = 4.7 Hz), 111.8 (d, J = 9.6 Hz), 110.7, 110.4, 104.6 (d, J = 23.4 Hz), 39.6. ^{19}F NMR (377 MHz, $CDCl_3$) δ −124.2.

*2.1.4.16. 3,3′-((4-Nitrophenyl)methylene)bis(6-chloro-1H-indole) (**5a**).* Brown semi-solid (109 mg, 76% yield); ^{1}H NMR (400 MHz, $CDCl_3$) δ 8.13 (dd, J = 17.5, 10.7 Hz, 4H), 7.46 (d, J = 8.5 Hz, 2H), 7.37 (s, 2H), 7.19 (d, J = 8.5 Hz, 2H), 6.98 (dd, J = 8.5, 1.3 Hz, 2H), 6.65 (d, J = 2.0 Hz, 2H), 5.91 (s, 1H). ^{13}C NMR (100 MHz, $CDCl_3$) δ 151.0, 146.7, 137.0, 129.4, 128.4, 125.1, 124.2, 123.8, 120.5, 120.3, 118.1, 111.3, 40.0.

*2.1.4.17. 3,3′-((4-Bromophenyl)methylene)bis(6-chloro-1H-indole) (**5b**).* Maroon semi-solid (125 mg, 81% yield); ^{1}H NMR (400 MHz, $CDCl_3$) δ 7.98 (s, 2H), δ 7.45–7.38 (m, 2H), 7.34 (d, J = 1.6 Hz, 2H), 7.21 (d, J = 8.5 Hz, 2H), 7.16 (d, J = 8.3 Hz, 2H), 6.97 (dd, J = 8.5, 1.8 Hz, 2H), 6.62 (dd, J = 2.4, 1.0 Hz, 2H), 5.75 (s, 1H). ^{13}C NMR (100 MHz, $CDCl_3$) δ 142.3, 137.03, 131.4, 130.3, 128.1, 125.3, 124.1, 123.6, 120.5, 120.2, 119.0, 111.1, 39.5. HRMS (ESI): calculated for $C_{23}H_{15}N_2Cl_2Br$ $[M + H]^+$ 468.9829, found 468.9874.

*2.1.4.18. 3,3′-((4-Chlorophenyl)methylene)bis(6-chloro-1H-indole) (**5c**).* Semi-solid (119 mg, 85% yield); ^{1}H NMR (400 MHz, $CDCl_3$) δ 7.95 (s, 2H), 7.33 (d, J = 1.8 Hz, 2H), 7.26–7.22 (m, 4H), 7.20 (d, J = 5.9 Hz, 2H), 6.96 (dd, J = 8.5, 1.8 Hz, 2H), 6.60 (dd, J = 2.4, 1.0 Hz, 2H), 5.76 (s, 1H). ^{13}C NMR (100 MHz, $CDCl_3$) δ 141.8, 137.0, 132.1, 129.9, 128.5, 128.1, 125.3, 124.1, 120.6, 120.2, 119.1, 111.1, 39.4. HRMS (ESI): calculated for $C_{23}H_{15}N_2Cl_3$ $[M + H]^+$ 425.0334, found 425.0379.

*2.1.4.19. 3,3′-((4-Fluorophenyl)methylene)bis(6-chloro-1H-indole) (**5d**).* Maroon semi-solid (130 mg, 85% yield); ^{1}H NMR (400 MHz, $CDCl_3$) δ 7.90 (s, 2H), 7.27 (d, J = 1.7 Hz, 2H), 7.16 (dd, J = 9.7, 5.8 Hz, 4H), 6.95–6.80 (m, 4H), 6.54 (dd, J = 2.3, 0.9 Hz, 2H), 5.71 (s, 1H). ^{13}C NMR (100 MHz, $CDCl_3$) δ161.53 (d, J = 244.3 Hz), 138.02 (d, J = 197.6 Hz), 130.01, 129.98 (d, J = 7.8 Hz), 128.10, 125.41, 124.11, 120.64, 120.20, 119.46, 115.17 (d, J = 21.3 Hz), 111.11, 39.31. ^{19}F NMR (377 MHz, $CDCl_3$) δ −116.76.

*2.1.4.20. (2S,3S,4R,5S)-2-(Acetoxymethyl)-6-(5-bromo-1H-indol-1-yl)tetrahydro-2H-pyran-3,4,5-triyl triacetate (**10**).* (130 mg, 80% yield); ^{1}H NMR (400 MHz, $CDCl_3$) δ 7.73 (d, J = 1.8 Hz, 1H), 7.32 (d, J = 1.8 Hz, 1H), 7.29 (d, J = 8.7 Hz, 1H), 7.23 (d, J = 3.4 Hz, 1H), 6.51 (d, J = 3.4 Hz, 1H), 5.57 (d, J = 8.8 Hz, 1H, H-1), 5.50 (t, J = 9.1 Hz, 1H), 5.44 (t, J = 9.2 Hz, 1H), 5.29 (t, J = 9.6 Hz, 1H), 4.30 (dd, J = 12.5, 4.8 Hz, 1H), 4.21–4.08 (m, 2H), 3.99 (ddd, J = 10.1, 4.8, 2.3 Hz, 1H), 2.15–1.97 (m, 12H). ^{13}C NMR (100 MHz, $CDCl_3$) δ 170.6, 170.1, 169.4, 168.7, 134.6, 130.7, 125.7, 125.2, 123.8, 113.9, 111.1, 103.8, 83.3 (C-1), 74.7, 73.1, 70.4, 68.0, 61.8, 20.7, 20.6, 20.5, 20.1. HRMS (ESI): calculated for $C_{22}H_{25}NO_9Br$ $[M + H]^+$ 526.0713, found 526.0710.

*2.1.4.21. (3S,4R,5R,6S)-2-(5-Bromo-1H-indol-1-yl)-6-(hydroxymethyl)tetrahydro-2H-pyran-3,4,5-triol (**11**).* (124 mg, 95% yield); ^{1}H NMR (400 MHz, MeOD) δ 7.57 (t, J = 2.0 Hz, 1H), 7.42–7.30 (m, 2H), 7.14 (dq, J = 8.8, 1.8 Hz, 1H), 6.37 (t, J = 2.7 Hz, 1H), 5.33 (dd, J = 9.1, 2.2 Hz, 1H, H-1), 3.83–3.73 (m, 2H), 3.64–3.58 (m, 1H), 3.53–3.44 (m, 2H), 3.42 (d, J = 9.1 Hz, 1H), 3.20 (p, J = 1.7 Hz, 1H). ^{13}C NMR (100 MHz, MeOD) δ 135.2, 130.8, 126.7, 124.0, 122.6, 112.7, 111.9, 101.6, 85.4 (C-1), 79.2, 77.5, 72.2, 69.9, 61.2. HRMS (ESI): calculated for $C_{14}H_{17}NO_5Br$ 358.0290, found 358.0293.

*2.1.4.22. (2S,3S,4R,5S)-2-(Acetoxymethyl)-6-(5-bromo-3-((5-bromo-1-((2S,3R,6R)-3,4,5 triacetoxy-6-(acetoxymethyl) tetrahydro-2H-pyran-2-yl)-1H-indol-3-yl)(4 fluorophenyl)-methyl)-1H-indol-1-yl)tetrahydro-2H-pyran-3,4,5-triyl triacetate (**12**).* Pale yellow semi-solid (70.591 mg, 64% yield); ^{1}H NMR (400 MHz, $CDCl_3$) δ 7.48 (s, 1H), 7.36–7.31 (m, 5H), 7.21–7.17 (m, 2H), 7.00 (t, J = 8.6 Hz, 2H), 6.71 (d, J = 7.1 Hz, 2H), 5.64 (s, 1H), 5.51–5.43 (m, 3H), 5.42–5.35 (m, 3H), 5.23 (d, J = 9.7 Hz, 2H, H-1), 4.33–4.21 (m, 3H), 4.17 (d, J = 2.2 Hz, 1H), 3.98–3.92 (m, 2H), 2.24–1.84 (m, 24H). ^{13}C NMR (100 MHz, $CDCl_3$) δ 170.7, 170.5, 170.1, 169.3, 162.1 (d, J = 337.6 Hz), 140.9, 134.9 (d, J = 23.7 Hz), 129.7 (d, J = 11.5 Hz), 125.5, 124.9, 122.2, 120.3, 115.4 (d, J = 21.5 Hz), 113.8, 111.5, 100.8, 83.6 (C-1), 74.7, 72.9, 70.8, 70.3, 67.9, 29.7, 20.6, 20.5, 20.0, 19.9. ^{19}F NMR (377 MHz, $CDCl_3$) δ −116.6. HRMS (ESI): calculated for $C_{52}H_{51}N_2O_{18}FBr_2$ $[M + H]^+$ 1157.1521, found 1157.1566.

*2.1.4.23. 6,6′-(((4-Fluorophenyl)methylene)bis(5-bromo-1H-indole-3,1-diyl))bis(2-(hydroxy-methyl)tetrahydro-2H-pyran-3,4,5-triol) (**13**).* Pale yellow semi-solid (63.5 mg, 90% yield). ^{1}H NMR (400 MHz, MeOD) δ 7.38 (dd, J = 8.8, 1.9 Hz, 2H), 7.34–7.27 (m, 2H), 7.22 (dd, J = 8.5, 5.4 Hz, 2H), 7.17–7.12 (m, 2H), 6.91 (t, J = 8.7 Hz, 2H), 6.83 (d, J = 2.5 Hz, 2H), 5.67 (s, 1H), 5.26 (d, J = 9.1 Hz, 2H, H-1), 3.76 (dd, J = 12.1, 2.1 Hz, 2H), 3.65 (td, J = 9.0, 2.4 Hz, 2H), 3.58 (ddd, J = 12.1, 5.8, 2.1 Hz, 2H), 3.44 (t, J = 8.9 Hz, 4H), 3.32 (td, J = 9.3, 3.6 Hz, 2H). ^{13}C NMR (100 MHz, MeOD) δ 161.5 (d, J = 243.1 Hz), 139.2, 135.9 (d, J = 6.9 Hz), 130.0, 129.9 (d, J = 8.0 Hz), 125.9, 124.3, 121.6, 118.3 (d, J = 9.1 Hz). 114.6, 114.4, 112.5, 112.2, 85.5 (C-1), 79.2, 77.6, 72.1, 69.9, 61.2, 38.7. ^{19}F NMR (377 MHz, MeOD) δ −118.8. HRMS (ESI): calculated for $C_{35}H_{35}N_2O_{18}FBr_2$ $[M + H]^+$ 821.0679, found 821.0721.

2.2. Biological evaluation

2.2.1. Chemicals. All the synthesized derivatives were stored at −20 °C with their dissolutions made in 100% dimethyl sulfoxide (DMSO) at a concentration of 20 mM. Amphotericin B, Alamar Blue, 3-(4,5-dimethylthiazol-2-yl)-2,5-diphenyltetrazolium bromide (MTT dye), and fetal bovine serum (FBS) were purchased from Himedia. The culture medium (M199 and DMEM) was purchased from Gibco and Himedia.

2.2.2. Parasite culture and cell line maintenance. Standard amphotericin B sensitive *L. donovani* strain DD8 (MHOM/IN/80/DD8) was maintained in M199 medium supplemented with 10% FBS, 25 mM HEPES buffer (pH 7.2), 2.2 g L^{-1} sodium bicarbonate, 100 mg L^{-1} penicillin, 100 mg L^{-1} gentamycin, and 100 mg L^{-1} streptomycin sulfate. The culture was initiated at 1×10^5 parasites per ml and grown at 24 ± 1 °C for 4–5 days before subculturing.[23] For the cytotoxicity experiments, the J774A.1 cell line was grown in DMEM medium prepared with 3.7 g L^{-1} sodium bicarbonate, 3.5 g L^{-1} D-glucose, 70 mg L^{-1} penicillin, 70 mg L^{-1} gentamycin, and 100 mg L^{-1} streptomycin sulfate.[24]

2.2.3. *In vitro* screening for anti-leishmanial activity. The *in vitro* anti-leishmanial activity assay was carried out on *L.*

donovani DD8 promastigotes grown at 24 ± 1 °C in M199 liquid medium supplemented with 10% heat-inactivated FBS. The effect of synthesized 3,3′-DIM derivatives on the viability of *L. donovani* DD8 cells was determined by the Alamar Blue cell viability assay.[25] Exponentially growing promastigote cells were collected and transferred into a 96-well plate (5×10^6 cells per well). 1 mM stock solution of each compound was prepared in DMSO. The cells were then incubated for 24 h in the presence of five different concentrations of 3,3′-DIM derivatives (100, 50, 25, 12.5, and 6.25 μM). Parasite viability was assessed using resazurin-based Alamar Blue dye with a final 20 μg ml^{-1} concentration. Optical density with an excitation wavelength of 550 nm and an emission wavelength of 590 nm was measured using a Tecan Infinite M200 pro multimode plate reader with amphotericin B as a standard drug. The inhibitory concentration (IC_{50}) value was determined using GraphPad Prism 8 (version 8.0.2). All results are calculated as the mean ± standard deviation of three independent measurements.

2.2.4. Cytotoxicity assay. The cytotoxicity of potent compounds was determined against the J774A.1 cell line by the MTT assay.[25,26] J774A.1 is a murine macrophage cell line derived from a tumor in female BALB/c mice.[27] Briefly, J774A.1 cells (2×10^4 cells per well) were cultured in DMEM complete medium, plated into a 96-well tissue culture plate and left overnight to adhere. After 24 hours, the cells were treated with compounds at different concentrations (100, 50, 30, 20, and 10 μM) in triplicate keeping the final DMSO concentration at 0.1%. DMSO was the negative control, and amphotericin B was the positive control. After 20 h of incubation, 20 μl MTT dye was added (2.5 mg ml^{-1} PBS) to each well, further incubating the plate at 37 °C for 4 hours. The experiment was terminated by adding 100 μl of DMSO to dissolve the formed formazan crystals. The optical density was measured at 570 nm using a microplate reader (Tecan Infinite M200). The cytotoxic concentration (CC_{50}) value was measured using GraphPad Prism 8 (version 8.0.2). All results are calculated as the mean ± standard deviation of three independent measurements.

2.2.5. Molecular docking procedure. DNA topoisomerases have emerged as a principal therapeutic target for various anti-leishmanial drugs.[28] As the literature survey points topoisomerase IB as the most likely target for bisindole compounds, we attempted to perform molecular docking of potent 3,3′-DIM analogs (free drug and glycosylated) to check for their binding affinities.[29] To perform the molecular docking experiments, the receptor crystal structure of leishmanial topoisomerase I protein (PDB ID: 2B9S) and human topoisomerase I (PDB ID: 1EJ9) was taken from the PDB. Molecular docking was performed using AutoDock Vina 1.1.2. The input was provided in the form of the receptor, ligand, and a configuration file consisting of information about the size and centers of the grid box, while the output was in the form of a list of poses ranked by a score that corresponds to the predicted binding energy (ΔG, kcal mol^{-1}). The exhaustiveness was set at 8, the number of binding modes was set at 9, and the energy range of all the binding poses was fixed at 3 kcal mol^{-1}. The docking potent 3,3′-DIM compound along with its glycoside against the macromolecular structures of the two enzymes (1EJ9 & 2B9S) and the RdRp was accomplished into the binding site residues inside a grid box with *X*, *Y*, and *Z* axes and dimensions adjusted to −1.762 Å × −0.363 Å × 35.035 Å (size: 60 × 60 × 60) for the human topoisomerase I DNA complex and 39.112 Å × 40.944 Å × 11.518 Å (size: 62 × 62 × 62) for the heterodimeric *L. donovani* topoisomerase I-vanadate-DNA complex, respectively. After molecular docking of ligands against these proteins, the best-docked poses of compounds and the interactions with the binding residues of the proteins were visualized using BIOVIA Discovery Studio Visualiser v21.1.0.20298.

2.2.6. Recombinant LdTOPILS purification. *Escherichia coli* BL21 (DE3) cells (500 ml) containing pET16bLdTOP1L and pET16bLdTOP1S plasmids were cultured and induced by 0.5 mM IPTG (isopropyl βD-thiogalactoside) once/till an OD_{600} of 0.6 was achieved and incubated at 22 °C for 12 hours. The culture was harvested by lysozyme and sonication followed by Ni-NTA-agarose column (Qiagen) based purification of LdTopILS. Purified enzyme fractions were collected and stored at −80 °C. The enzyme activity of the purified fractions was assayed with the pHOT1 plasmid DNA as the substrate in a molar ratio of 3 : 1 and analyzed by agarose gel electrophoresis.

2.2.7. Plasmid relaxation assay. The activity of the synthesized 3,3′-DIM derivatives and their glycosides on the recombinant *Leishmania donovani* topoisomerase IB (LdTopILS) protein was investigated by analyzing the formation of supercoiled monomers *versus* relaxed monomers of the pHOT1 DNA in agarose gel electrophoresis. A relaxation assay was carried out as described previously.[30] Briefly, recombinant LdTopILS was incubated with the relaxation buffer (25 mM Tris-Cl, pH 7.5), 5% glycerol, 50 mM potassium chloride, 0.5 mM dithiothreitol, 10 mM magnesium chloride, and 30 μg ml^{-1} bovine serum albumin, supercoiled pHOT1 DNA along with either camptothecin (CPT, 60 μM, positive control) or DMSO (4% v/v, solvent control) or the synthesized 3,3′-DIM derivatives at the indicated concentrations for 25 min at 37 °C. After incubation, the samples were separated on 1% agarose gel, followed by quantification of the relaxed and supercoiled monomers using EtBr staining (0.5 mg ml^{-1}) and the Gel Doc system under UV illumination (G-Box Chemi-XRQ – GeneSys software).

2.2.8. Statistical analysis. Statistical analysis was carried out using GraphPad Prism 8 (version 8.0.2) software (GraphPad Software Inc., La Jolla, CA, USA). Student's *t*-test was used to estimate the statistical significance of the differences between groups. Differences between groups were considered statistically significant when the *p*-value was less than 0.05 ($*p < 0.05$; $**p < 0.01$; $***p < 0.001$).

3. Results

3.1. Synthesis of 3,3′-DIM derivatives and their anti-leishmanial effect on *L. donovani* promastigotes

The electrophilic substitution reactions of indoles with benzaldehydes, using montmorillonite clay in DCM, generated 3,3′-DIMs **2a–5d** in good yields (Scheme 1 and Table 1). All the synthesized 3,3′-DIM derivatives were evaluated for anti-leishmanial activity. Several compounds showed promising anti-leishmanial activity, as depicted in Table 1. Among the synthesized 3,3′-DIM derivatives, compounds **2d**, **3d**, and **4a** showed IC_{50} values in the range of 30–36 μM. The IC_{50} value of standard amphotericin B used in experiments was 0.4 ± 0.06 μM, which corroborated with previous studies.[31,32] From the observations, it was concluded that the derivatives having either fluoro indole or 4-fluoro benzaldehyde seem more potent.

Our subsequent strategy involved glycosylating the bioactive DIM derivative **3d**. The *N*-glycosylated DIM derivatives used in this study were synthesized by following the previously known literature procedure.[13] Briefly, using sodium cyanoborohydride, 5-bromoindole (**6**) was reduced to the corresponding indoline (**7**) using acetic acid. This 5-bromoindoline (**7**) was then converted to the corresponding glycosyl-indoline (**8**) with the addition of D-glucose in a mixture of ethanol and water. Compound **8** formed was acetylated in the presence of pyridine and acetic anhydride, resulting in compound **9**, which was further aromatized with DDQ to obtain compound **10**. 5-bromoindole derivative **9** aromatization to **10** was confirmed by ^{1}H NMR spectral δ values of 6.51 and 7.23 ppm and ^{13}C NMR spectral δ values of 103.8 and 125.2 ppm. Synthesis of glycosylated DIM **12** in quantitative yield was thereafter achieved using compounds **10** and 4-fluorobenzaldehyde. The formation of the β-*N*-glycosidic link in compound **12** was confirmed by the appearance of an anomeric doublet peak with a coupling constant (J) of 9.7 Hz for anomeric hydrogen (H-1) at a δ value of 5.23 ppm in the ^{1}H-NMR spectrum and the corresponding peak of anomeric carbon atoms in the ^{13}C-NMR spectrum at 83.6 ppm. Finally, acetylated compounds **10** and **12** were deprotected in the presence of sodium methoxide in methanol, resulting in desired compounds **11** and **13**, respectively (Scheme 2). The formation of the β-*N*-glycosidic link in compound **13** was confirmed by the

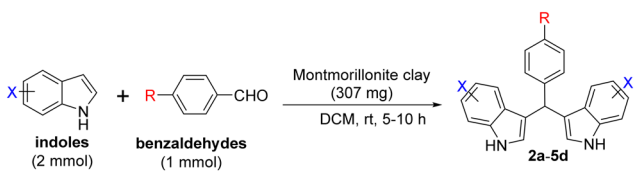

Scheme 1 Synthesis of 3,3′-DIM derivatives using varied substituted indoles and aldehydes. Reagents and conditions: indoles (2 mmol), benzaldehydes (1 mmol), montmorillonite clay (307 mg), DCM, room temperature, 5–10 h.

Table 1 3,3′-DIM derivatives from Scheme 1 and their potency on *L. donovani* promastigotes

Compound no.	X=	R=	% yield[a]	IC_{50}[b] (μM)
2a	H	$-NO_2$	83	>100
2b	H	–Br	85	46.98 ± 2.18
2c	H	–Cl	64	57.12 ±1.76
2d	H	–F	76	36.20 ± 2.09
2e	H	$-CH_3$	78	54.29 ± 2.53
2f	H	$-OCH_3$	64	54.90 ± 2.47
2g	H	$-SCH_3$	72	>100
3a	5-Br	$-NO_2$	79	48.47 ± 1.89
3b	5-Br	–Br	85	>100
3c	5-Br	–Cl	81	41.80 ± 1.74
3d	5-Br	–F	72	34.81 ± 1.59
3e	5-Br	$-CH_3$	81	59.20 ± 2.34
3f	5-Br	$-OCH_3$	85	>100
3g	5-Br	$-SCH_3$	76	>100
4a	5-F	–Cl	72	31.38 ± 1.53
5a	6-Cl	$-NO_2$	86	48.35 ± 2.18
5b	6-Cl	–Br	81	74.27 ± 2.29
5c	6-Cl	–Cl	85	53.19 ± 2.16
5d	6-Cl	–F	85	>100

[a] Isolated yield. [b] IC_{50} against *L. donovani*.

appearance of an anomeric doublet peak with a coupling constant (J) of 9.1 Hz for anomeric hydrogen (H-1) at a δ value 5.26 ppm in the ^{1}H-NMR spectrum, which is further supported by the appearance of a corresponding peak of anomeric carbon atoms in the ^{13}C-NMR spectrum at 85.5 ppm. *In vitro*, the anti-leishmanial activity of the synthesized glycosylated compounds **12** and **13** was 29.11 ± 1.83 μM and 27.91 ± 1.37 μM, respectively. Further, the potent DIM derivatives **2d**, **3d**, and **4a** and glycosylated DIM **13** were screened to check their cytotoxicity against the J774A.1 cell line.

3.2. Structure–activity relationship (SAR) analysis

We aimed to establish a SAR of our synthesized 3,3′-DIM derivatives in accordance with the anti-leishmanial activity of the corresponding compounds in terms of IC_{50} values (Table 1). The anti-leishmanial activities of compounds **2a–2g** derived from unsubstituted indole and various substituted benzaldehydes revealed that 3,3′-DIM derivatives are more active if synthesized from benzaldehydes carrying electron-withdrawing substituents (**2b–2d**) than electron donating groups (**2e–2g**). Among electron-withdrawing halogen substituents in **2b–2d**, fluorine substitution (**2d**) is the most active with an IC_{50} value of ~36 μM. Compound **2a** synthesized from benzaldehyde having a strong electron-withdrawing substituent like the nitro group was found to be inactive. In the case of compounds **2e–2g**, which were synthesized from electron-donating benzaldehydes, the replacement of the methyl group (**2e**) with a strong electron-donating methoxy group (**2f**) failed to contribute any considerable improvement in the IC_{50} value. Replacement of the methoxy group (**2f**) with a thiomethyl group (**2g**) resulted in a complete loss in activity. Further, we have studied the

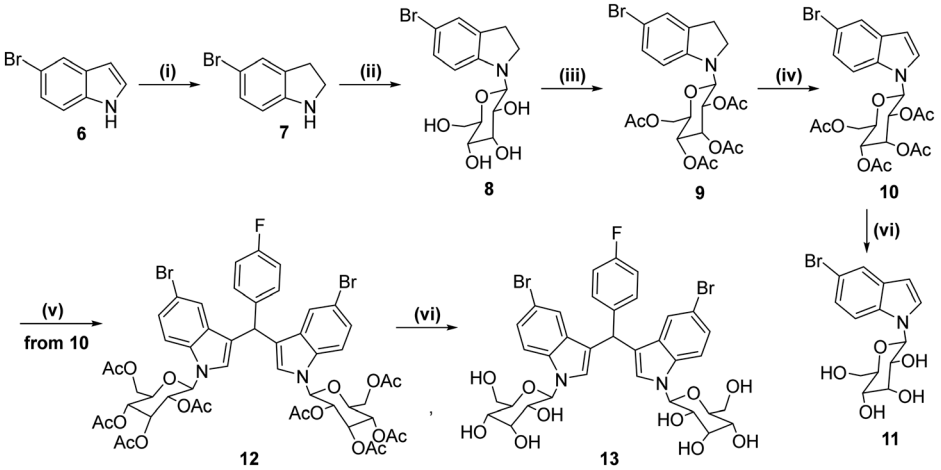

Scheme 2 Synthesis of 3,3′-DIM *N*′-linked glycoconjugate (**13**). Reagents and conditions: (i) sodium cyanoborohydride, AcOH, 12 °C, N_2 atm., 2 h; (ii) D-glucose, EtOH, H_2O, 90 °C, 24 h; (iii) Ac_2O, pyridine, r.t., 24 h; (iv) DDQ, dioxane, r.t., 24 h; (v) iodine, 4-fluorobenzaldehyde, 0 °C–r.t., 30 s; and (vi) NaOMe, MeOH, r.t., 30 min.

effect of substituted indole on the anti-leishmanial activity. We have synthesized compounds **3a**–**3g** using 5-bromoindole and benzaldehydes. Again, we have observed that 3,3′-DIM derivatives synthesized from benzaldehydes carrying electron-withdrawing substituents (**3a**, **3c**, and **3d**) are more active than those carrying electron donating groups (**3e**–**3g**), and compound **3d** with fluoro substitution was the most potent with an IC_{50} value of ~34 μM. Also, we have observed that 3,3′-DIM derivatives synthesized from 5-bromoindole (**3a**, **3c**, and **3d**) showed improved biological activity compared to those synthesized from unsubstituted indole (**2a**, **2c**, and **2d**). Further, the 3,3′-DIM derivative derived from 5-fluoroindole (**4a**) resulted in better anti-leishmanial activity than that derived from 5-bromoindole (**3c**). Compounds **5a**–**5d** synthesized from 6-chloroindole were comparable (**5a** *vs.* **3a**, **5b** *vs.* **3b**) and less (**5c** *vs.* **3c**, and **5d** *vs.* **3d**) active than those synthesized from 5-bromoindole *i.e.*, **3a**–**3d**. To find out whether glycosylation brings any change in the activity of active 3,3′-DIM, we synthesized the *N*-glycosyl derivative of **3d** *i.e.*, compound **13** (Scheme 2). From the IC_{50} values of these compounds **3d** (34.81 μM) and **13** (27.91 μM), we concluded that glycosylation of 3,3′-DIM caused enhancement in activity.

3.3. Cytotoxic effect of bisindoles on the J774A.1 cell line

Reduction of MTT by actively dividing cells constitutes a suitable parameter to assess the viability in an extensive range of cell lines.[25] The effect of bisindoles on MTT reduction was assessed to evaluate their cytotoxicity. The cytotoxicity of potent non-glycosylated DIM (**2d**, **3d**, and **4a**) and glycosylated DIM **13** was assessed in the J774A.1 macrophage cell line in terms of drug concentration required to reduce cell toxicity. The results at different concentrations of testing are compiled in Table 2. Non-glycosylated DIM **2d**, **3d**, and **4a** showed percentage viability in the 26–40% range at 10 μM concentration. Glycoside DIM **13** showed a percentage viability of 96.25% at 10 μM drug concentration, which is significantly higher than its non-glycosylated derivative **3d**. Similarly, at 20 μM concentration, the percentage viability for non-glycosylated DIM derivatives was 20–35% and the glycosylated DIM derivative (**13**) showed a percentage viability of ~80%. Also, at higher concentrations (30 and 50 μM) a similar pattern of percentage viability in the cell line was observed. A dose-dependent cytotoxicity comparison of non-glycoside (**3d**) and glycoside DIM derivatives (**13**) is presented in Fig. 2. The CC_{50} value of the glycosylated molecule (**13**) was ~20 times higher as compared to that of the non-glycosylated molecule (**3d**). These results suggest that glycosylation significantly reduced the toxic effects of the DIM derivatives.

3.4. Molecular docking results

The molecular docking results of biologically active compounds (**2d**, **3d**, **4a**, **12**, and **13**) are compiled in Table 3.

Table 2 Difference in cytotoxic effects of glycosylated and non-glycosylated compounds on the J774A.1 cell line

Compound no.	Percentage viability on the J774A.1 cell line				
	50 μM	30 μM	20 μM	10 μM	CC_{50} (μM)
2d	15.89 ± 1.74	19.81 ± 1.64	20.05 ± 1.07	26.23 ± 1.24	5.71 ± 0.31
3d	21.73 ± 2.21	30.34 ± 2.17	34.28 ± 1.53	39.59 ± 1.83	4.45 ± 0.84
4a	26.14 ± 2.42	32.04 ± 1.98	33.53 ± 1.74	40.15 ± 2.01	4.51 ± 1.17
13	69.77 ± 2.38	70.11 ± 2.09	81.05 ± 2.13	96.25 ± 2.37	89.15 ± 2.39

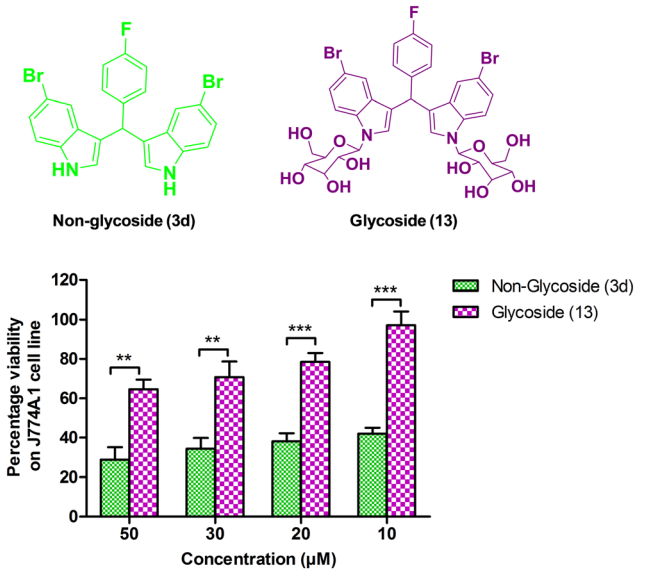

Fig. 2 Differential effects of non-glycoside and glycoside DIM derivatives on reduced cytotoxicity. All results are calculated as the mean ± standard deviation of three independent measurements. **, $p < 0.01$; ***, $p < 0.001$; by Student's *t*-test using GraphPad Prism.

We have observed that compound **4a** showed a higher binding affinity for human and leishmanial topoisomerase when compared with **2d** and **3d**. The same result was observed in the *in vitro* assay in which compound **4a** was found to be more active than other non-glycosylated DIM derivatives (Table 1). In biological studies, we have observed that glycosylated DIM **13** showed reduced cytotoxicity compared to its non-glycosylated counterpart **3d**. On proceeding with molecular docking studies, the **3d** (non-glycosylated DIM) binding energy against human and leishmanial topoisomerase was found to be −10.5 and −10.5, respectively (Fig. 3A). In contrast, compound **13** (a glycosylated derivative of **3d**) showed a lower binding energy of −11.8 and −11.3 with human and leishmanial topoisomerase, respectively (Fig. 3B). The protein–ligand interaction study of compound **13** with human topoisomerase is involved in five H-bond interactions, one with Asn722, Asp440, and DNA cytosine (DC) and two with DNA thymine (DT). The same glycoside **13** showed three H-bond interactions with leishmanial topoisomerase at Ser244, Gln175, and DT. The 3D representation (Fig. 4) depicted the binding interactions differentiating non-glycoside from glycoside. Also, compounds **3d** and **13** displayed various interactions like pi–pi interactions, van der Waals interactions, halogen bonds, conventional hydrogen bonds, and C–H bonding interactions with key amino acid residues.

Table 3 Binding affinity of bisindoles against the human and leishmanial topoisomerase IB enzyme

Compound no.	Affinity (kcal mol^{-1})	
	Human top I	Leishmanial top IB
2d	−10.1	−10.0
3d	−10.5	−10.5
4a	−11.1	−11.1
12	−8.2	−8.1
13	−11.8	−11.3

3.5. Plasmid relaxation assay

Topoisomerase inhibitors are classified into two types, *i.e.*, type 1 inhibitors or 'topoisomerase-poisons' and type 2 inhibitors or 'catalytic inhibitors'.[33] Catalytic inhibitors are competitive inhibitors that bind only to the topoisomerase enzyme and inhibit its activity. On the other hand, topoisomerase poisons bind to the enzyme–substrate (topoisomerase–DNA) complex and stabilize it, leading to the formation of a topoisomerase I–DNA cleavable complex (Top cc). This formation of irreversible double-strand breaks is the basis of cytotoxicity which increases with the cellular levels of the topoisomerase enzyme. Therefore, class I inhibitors are considered to be more potent as compared to class II inhibitors.

In this study, we performed the plasmid relaxation assay under standard conditions to check the inhibitory potential of the potent 3,3′-DIM derivatives and synthesized glycosides against LdTopILS. Recombinant LdTopILS was isolated and purified as described in the previous section (2.4). This recombinant LdTopILS was incubated with the plasmid DNA at a molar ratio of 3 : 1 under standard assay conditions. Under these conditions, LdTopILS is able to relax the supercoiled plasmid substrate and form topoisomers (Fig. 5, lane 2). DMSO was used as a solvent control (4% v/v) to check its effect on the activity of LdTopILS. However, no difference in the topoisomerase activity was observed in the presence of DMSO (Fig. 5, lane 3). Camptothecin (CPT), a potent topoisomerase poison of LdTopILS, completely inhibits the catalytic activity of the enzyme at 60 μM, because of which the substrate DNA fails to be in relaxed/topoisomers form and hence the supercoiled monomer of the substrate is obtained (Fig. 5, lane 4). Synthesized glycosylated and non-glycosylated DIM derivatives were used at a concentration of 500 μM to check the effect of compounds on the catalytic activity of the LdTopILS enzyme. Lanes 5–9 were loaded with potent non-glycosylated analogs, while lanes 10–15 contained glycosylated analogs (Fig. 5). The experimental results suggest that non-glycosylated DIM derivatives had no significant inhibitory effect on the LdTopILS enzyme. In contrast, glycosylated DIM derivatives were found to inhibit the LdTopILS enzyme significantly. The results showed that DIM glycosides **12** and **13** completely inhibited (100%) the LdTopILS activity as the supercoiled monomers were observed only for these DIM analogs (Fig. 5, lanes 14 and 15) similar to that of CPT. Moreover, DIM glycosides **10** and **11** inhibited more than 90% of the catalytic activity of LdTopILS (lanes 10 and 12). However, bromo-substituted glycosides (lanes 11 and

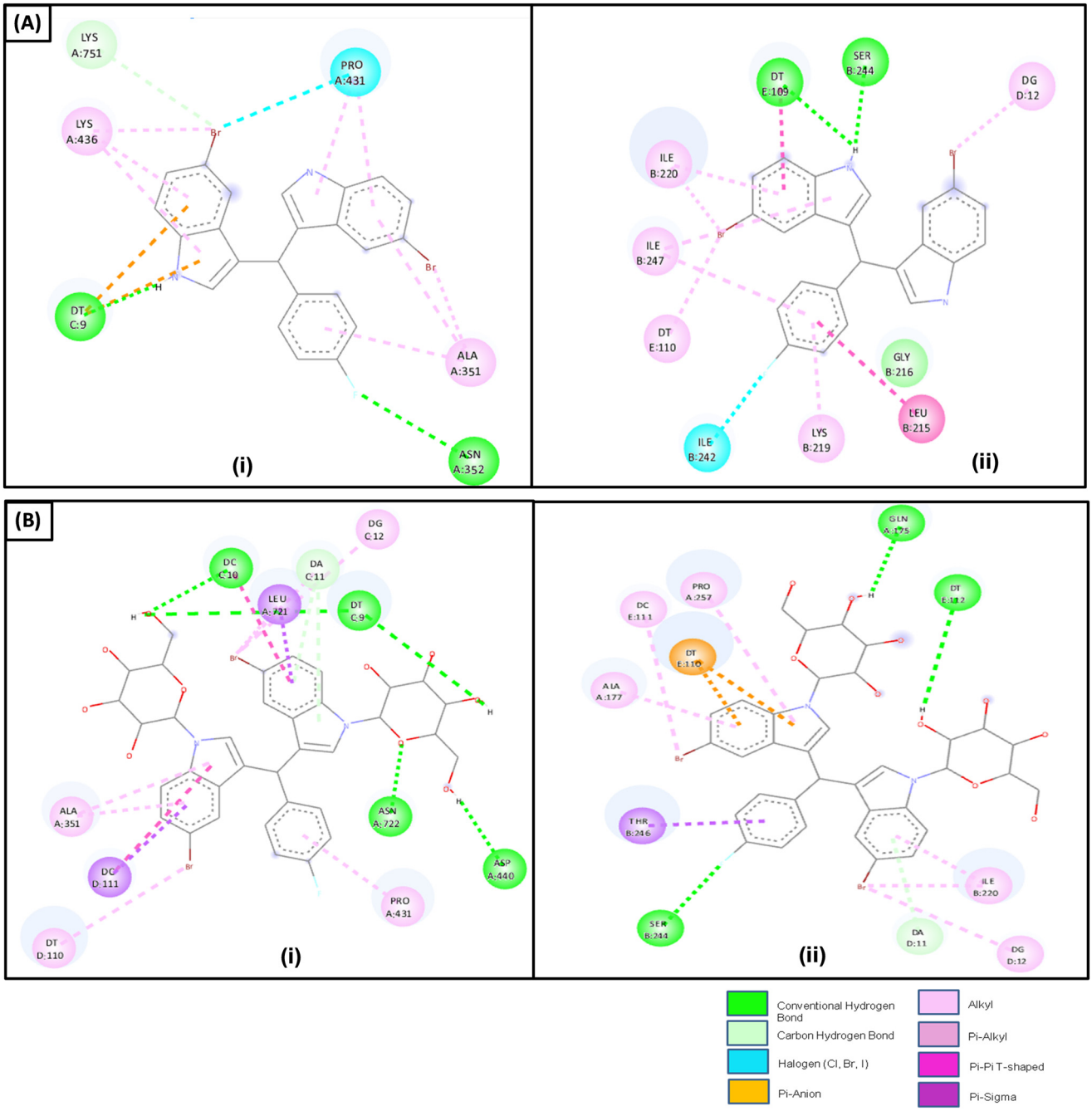

Fig. 3 Molecular docking analysis of non-glycoside and glycoside DIM derivatives. (A) Non-glycosylated compound **3d** docked with the human (i) and leishmanial (ii) topoisomerase enzyme. (B) Glycosylated compound **13** docked with the human (i) and leishmanial topoisomerase (ii) enzyme.

13) only partially inhibited the enzyme, as both the topoisomers and the supercoiled monomers of the plasmid DNA were observed. Based on the above observations, DIM glycosides (**11**, **12**, and **13**) were further analyzed for their inhibitory activity at lower concentrations (100, 200, and 400 μM). At 400 μM, DIM glycosides **12** and **13** caused complete inhibition of the enzyme (Fig. 6, lanes 7 and 10), while DIM glycoside **11** showed partial inhibition of LdTopILS at the same concentration (Fig. 6, lane 13). Furthermore, it was observed that fluoro-substituted DIM glycosides **12** and **13** were found to be potent inhibitors of LdTopILS.

4. Discussion

The parenteral drug therapy used for leishmaniasis is quite unsatisfactory and is flawed by various toxic side effects, longer treatment duration, and exorbitant prices. To counteract these conventional drawbacks and increasing cases of drug resistance, new anti-leishmanial drugs are

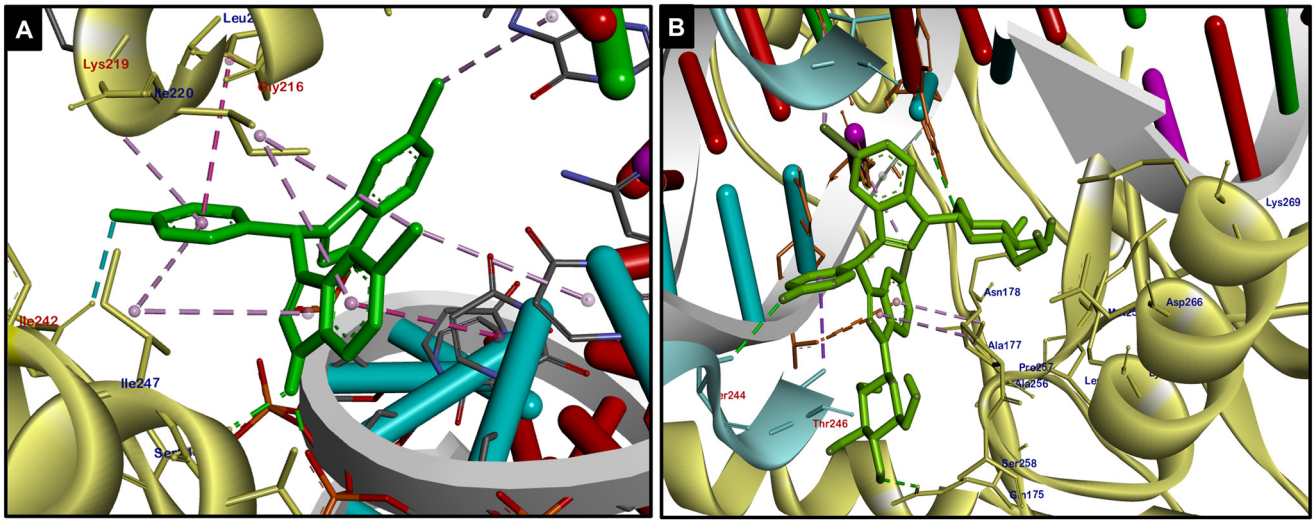

Fig. 4 3D representation of non-glycoside DIM **3d** (A) and glycoside DIM **13** (B) with leishmanial topoisomerase.

urgently needed. In the present study, we have shown that bisindoles constitute a privileged heterocyclic moiety that forms the core of a large number of synthetic compounds and could act as potent growth inhibitors of the *Leishmania* parasite. Among different classes of bisindoles, 3,3′-DIM derivatives have gained much attention as potent chemotherapeutic agents. Substantial previous literature studies have reported that 3,3′-DIM compounds exhibit immense pharmacological properties such as anti-bacterial, anti-fungal, and anti-proliferative.[8,34,35] This major component 3,3′-DIM is obtained from *Brassica* cruciferous plants such as cabbage, broccoli, brussels sprouts, cauliflower, *etc.* Roy's group,[10] for the first time in *Leishmania* parasites, reported that 3,3′-DIM acts as a potent topoisomerase I poison and induces programmed cell death by inhibiting the mitochondrial H^+-ATP synthase. Later the same group suggested that 3,3′-DIM inhibits the growth of the *Leishmania* parasite in a non-competitive manner by preventing strand religation and inducing DNA fragmentation.[36] Bharate's group[8] also synthesized 3,3′-DIM derivatives using an Fe-pillared interlayered clay catalyst and reported them to show promising anti-leishmanial, anti-fungal, and anti-bacterial activities.

In the search for new drugs to enhance the drug discovery process, the concept of glycosylation has been quite exploited. It has been well documented that addition of saccharide components adds some gratifying characteristics to free drugs and helps in improving their bioactivity, safety, and efficacy. This can be explained based on the configurational, conformational, and electronic properties imparted by them to the parent molecule. This in turn influences the pharmacological and pharmacokinetic profile

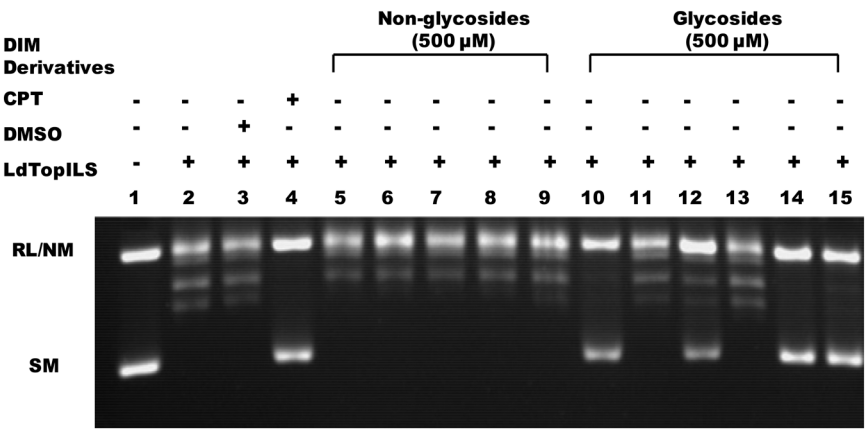

Fig. 5 The inhibition of LdTopILS activity by synthesized DIM derivatives. Analysis was performed using agarose gel electrophoresis by mixing the enzyme and pHOT1 DNA substrate at a molar ratio of 3 : 1 along with CPT (60 μM), DMSO (4% v/v), and the potent DIM derivatives (500 μM). Lanes 5–9 contained non-glycosylated DIM derivatives in the order **4a**, **3d**, **2d**, **3c**, and **2b** while lanes 10–15 contained glycosylated DIM derivatives. Lanes 10 and 12 represent compounds **10** and **11**. Lanes 11 and 13 represent bromo-substituted glycosides. Lanes 14 and 15 consist of glycosides **12** and **13**. These were quantitated and visualized by EtBr (0.5 mg ml^{-1}) staining and the Gel Doc system (G-Box Chemi-XRQ – GeneSys software). CPT – camptothecin; RL/NM – relaxed/nicked monomer; SM – supercoiled monomer.

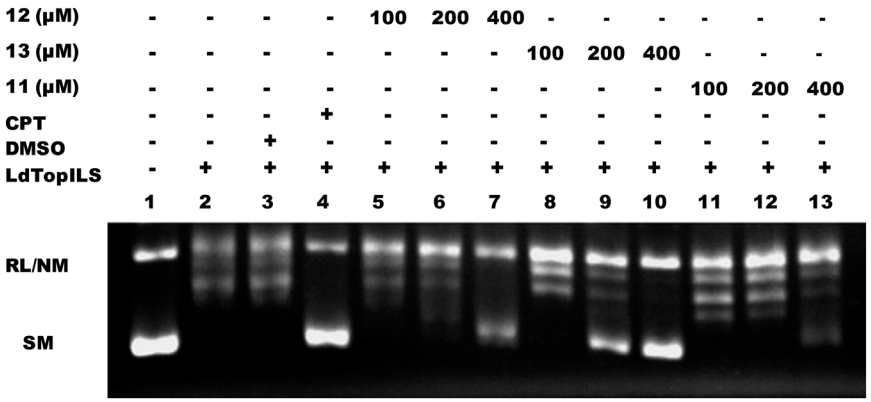

Fig. 6 The inhibition of LdTopILS activity by glycosylated DIM derivatives **11**, **12**, and **13** at lower concentrations. Analysis was performed using agarose gel electrophoresis by mixing the enzyme and pHOT1 DNA substrate at a molar ratio of 3 : 1 along with CPT (60 μM), DMSO (4% v/v), and the glycosylated DIM derivatives **11**, **12**, and **13** (100, 200, and 400 μM). These were quantitated and visualized by EtBr (0.5 mg ml^{-1}) staining and the Gel Doc system (G-Box Chemi-XRQ – GeneSys software). CPT – camptothecin; RL/NM – relaxed/nicked monomer; SM – supercoiled monomer.

of the targeted molecules to determine their specificity at tissue, cellular or molecular levels. Garg's group[37,38] observed the effect of galactosylated liposomes on the hepatic toxicity, cellular uptake, and pharmacokinetics of stavudine and azidothymidine. They found that stavudine entrapped within galactosylated liposomes showed no hematological and hepatic toxicity compared to free stavudine. Gulati's group[11] employed a similar concept of glycoconjugation to synthesize tacrine-linked triazole derivatives. Glycoside-rich fractions were found to inhibit the acetylcholinesterase enzyme with reduced hepatotoxicity. Sharma's group[13] synthesized *N*-glycoside derivatives of 3,3′-DIM exhibiting potent anti-proliferative activity. The study reported that glycosylation increased the efficacy of 3,3′-DIM derivatives and induced apoptosis by arresting the cells in the G_1 phase of the cell cycle. A study by Oda's group[39] evaluated the effect of glycosylation in drug delivery systems. They developed a glycoconjugate between D-galactose and β-cyclodextrin and found that the conjugate with the saccharide moiety served as a successful module for the efficient delivery of drug doxorubicin to the target site. Another study by Pukanud's group[40] developed acyclovir by liposome entrapment with sugar mannose. The mannosylated drug was found to have higher *in vitro* absorption than conventional acyclovir. Their study suggested that the addition of glycan to the free drug acyclovir resulted in increased bioadhesive properties of the drug and helped in enhancing the oral drug delivery system. Thus, the promise held by carbohydrates in the drug discovery process along with the recent developments in glycochemistry and glycobiology has inspired us to glycosylate the bioactive analogs of 3,3′-DIM for the development of effective drug candidates and promising anti-leishmanial lead compounds. Keeping all these aspects in view, we designed novel analogues of bisindolylmethanes for our present study, bringing in three modifications in the structure: (i) keeping the core bisindolylmethane scaffold intact and using different electron donating or withdrawing groups, (ii) changing the substituent on the aromatic portion of indole, and (iii) using two identical saccharide components with both nitrogens of a bisindolyl moiety.

Further, to discover inhibitors that translate from preclinical to clinical candidates, the identification of a selective drug target is a crucial step. Among various biological catalysts established as potential cellular targets, DNA topoisomerases have emerged as a principal therapeutic target for various infectious diseases, including leishmaniasis. The enzyme is found to have an unusual bi-subunit structure distinct from human counterparts in terms of biological properties and preferential sensitivity to many therapeutic agents, bringing a new twist to topoisomerase research. Due to its unique heteromeric feature, *L. donovani* topoisomerase 1B has been projected as an attractive target for anti-leishmanial inhibitor discovery. This ubiquitous enzyme works by a generalized three-step reaction: (i) binding of the enzyme to the substrate DNA, (ii) cleavage of one strand by a trans-esterification reaction allowing the other strand to pass through it and (iii) strand religation and turnover of the enzyme. In this study, we have developed a simple and efficient protocol for the synthesis of 3,3′-DIM derivatives targeting leishmanial topoisomerase IB aimed at reducing cytotoxicity. We tried to link it with another promising approach of glycoconjugation to study how glycosylated groups work differently from non-glycosylated ones. The biological evaluation revealed that acetylated and deacetylated sugars have different binding interactions with the topoisomerase 1B enzyme. Deacetylated glycoside (**13**) is more potent in enzyme inhibition than the acetylated one (**12**). Further, cytotoxicity analysis of glycosylated and non-glycosylated compounds showed that the glycosylated derivative was found to have significantly reduced toxic effects on the J774A.1 cell line. Experimental results supported the *in silico* studies by displaying significant

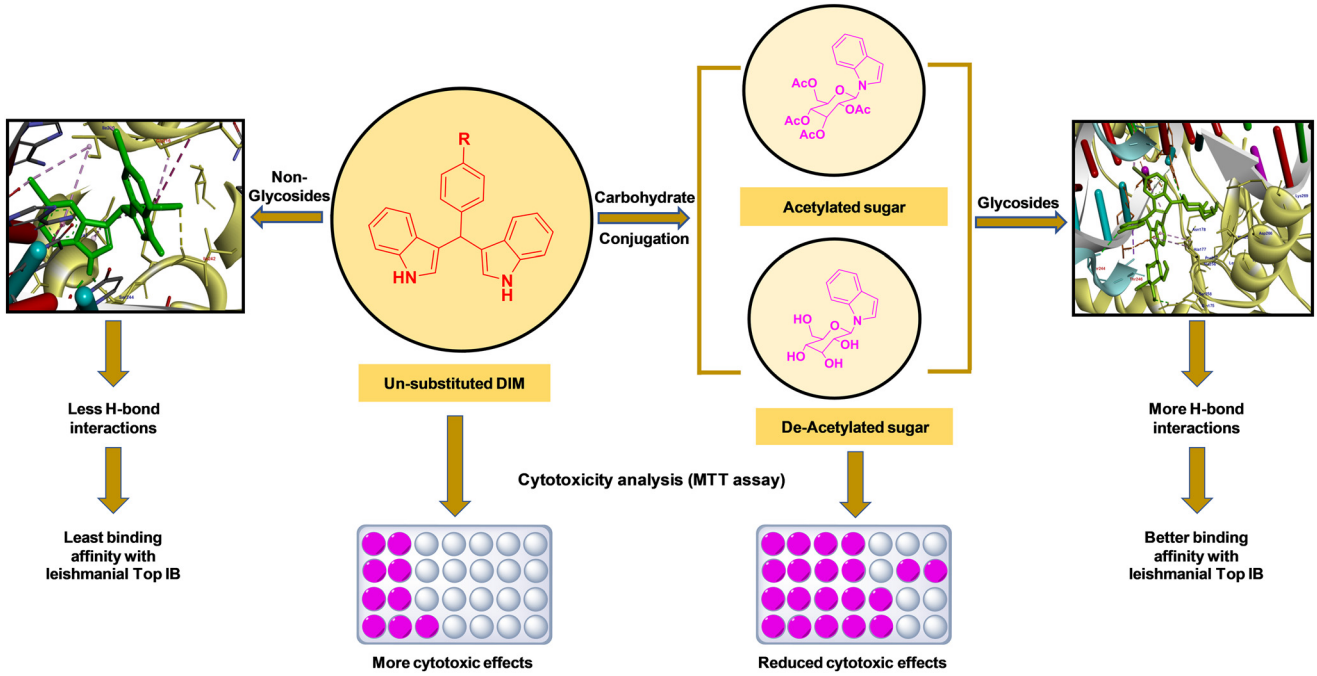

Fig. 7 Schematic representation of experimental outcomes from the present work.

protein–ligand interactions of glycosides with the target protein. They were found to occupy the binding site *via* pi–pi interactions, van der Waals interactions, halogen bonds, conventional hydrogen bonds, and carbon–hydrogen bonding interactions with some key amino acid residues. From the above observations, one can relate that *in vitro* analysis and computational predictions should go hand in hand to avoid toxicity issues later in the drug development process. Fig. 7 represents the overall summary of the present research work. This ample evidence relates to the fact that this concept of glycoconjugation should be worked upon to improve conventional therapeutics in the up-gradation of toxicity properties. An intense emphasis should be placed on developing glycosylated strategies to selectively and preferentially assist in developing a safe, effective, and stable formulation. Therefore, the glycosylation approach holds great promise for future clinical diagnostic and therapeutic applications and can be a valuable arsenal in combating dreadful diseases. Furthermore, it can be stated that glycosylation contributes significantly to reducing cytotoxicity, thus an integrated approach is required to harness glycosylation to overcome the existing therapeutic barriers in the drug-designing process and production of optimal and consistent therapeutic drugs for bringing better anti-leishmanial drug entities in the near future.

5. Concluding remarks

In summary, we have developed a simple and efficient protocol for the synthesis of structurally diverse 3,3′-DIM derivatives. Among all the tested compounds, fluorophenyl substituted derivatives were found to exhibit potent anti-leishmanial activity against *L. donovani* parasites. Enzyme inhibition studies suggested that 3,3′-DIM stabilizes topoisomerase I–DNA cleavable complex formation by hindering the DNA relaxation activity, ultimately inhibiting the parasitic replication and transcription leading to apoptotic cell death. Further, the addition of a sugar moiety to these free inhibitors resulted in reduced cytotoxicity against the J774A.1 macrophage cell line. Thereafter, molecular docking displayed better binding efficiency of glycosides with the target enzyme in comparison with non-glycosides. The study results also suggest that despite having a significant effect in reducing the cytotoxicity, the glycosylation approach did not result in considerable change in anti-leishmanial activity. Though the IC_{50} values for the glycosylated molecules were on the lower side as compared to those for the non-glycosylated molecules, significant reduction was not observed. Further, a major drawback of glycosylation that we came across is that the synthesis procedure is very tedious and time-consuming. It takes a multi-step reaction to synthesize one glycoside and purification of the glycoside for obtaining the final compound is laborious. As this is the first time we are checking the effect of glycosylated 3,3′-DIM molecules on growth inhibition of the *Leishmania* parasite and very little literature has been reported in this context, giving any finalized statement with just one study won't justify the concept. We are still into exploring this concept using different scaffolds. Further research is still needed to understand the biology of glycosylation and its fundamental effects on physicochemical and pharmacological properties.

Author contributions

PK – synthesized the bisindole and glycoside derivatives, performed the biological assays, writing – original draft. SB – analyzed and compiled the spectral data, DK – contributed to the biological experiments. PS and DKS – synthesized the glycoside, performed and compiled the *in silico* work. AD and AR – performed and compiled the enzyme activity work. KS and DM – conceptualization, resources, software, writing – original draft, review & editing, and supervision. All authors have read and approved the final version of the manuscript.

Conflicts of interest

The authors confirm that this article has no conflict of interest.

Acknowledgements

Kuljit Singh acknowledges the Department of Science & Technology – Science and Engineering Research Board (DST-SERB), New Delhi, for a Startup Research Grant (Grant No. SRG/2021/000293). Parampreet Kour (Junior Research Fellow) highly acknowledges the financial assistance in the form of fellowship support from DST-SERB. We also acknowledge the technical support from the central instrumentation facility of CSIR-IIIM, Jammu. The institutional manuscript communication number is CSIR-IIIM/IPR/00542.

References

1 S. Mann, K. Frasca, S. Scherrer, A. F. Henao-Martínez, S. Newman, P. Ramanan and J. A. Suarez, *Curr. Trop. Med. Rep.*, 2021, **8**, 121–132.
2 S. Burza, S. L. Croft and M. Boelaert, *Lancet*, 2019, **393**, 872–873.
3 D. Kumari and K. Singh, *Int. Immunopharmacol.*, 2022, **102**, 108400.
4 D. Kumari, S. Perveen, R. Sharma and K. Singh, *Eur. J. Pharmacol.*, 2021, **910**, 174436.
5 K. Singh, G. Garg and V. Ali, *Curr. Drug Metab.*, 2016, **17**, 897–919.
6 D. Kumari, S. Mahajan, P. Kour and K. Singh, *Life Sci.*, 2022, **306**, 120829.
7 M. Taha, I. Uddin, M. Gollapalli, N. B. Almandil, F. Rahim, R. K. Farooq, M. Nawaz, M. Ibrahim, M. A. Alqahtani and Y. A. Bamarouf, *BMC Chem.*, 2019, **13**, 1–12.
8 S. B. Bharate, J. B. Bharate, S. I. Khan, B. L. Tekwani, M. R. Jacob, R. Mudududdla, R. R. Yadav, B. Singh, P. Sharma and S. Maity, *Eur. J. Med. Chem.*, 2013, **63**, 435–443.
9 S. M. Kim, *Int. J. Mol. Sci.*, 2016, **17**, 1155.
10 A. Roy, A. Ganguly, S. BoseDasgupta, B. B. Das, C. Pal, P. Jaisankar and H. K. Majumder, *Mol. Pharmacol.*, 2008, **74**, 1292–1307.
11 H. K. Gulati, S. Choudhary, N. Kumar, A. Ahmed, K. Bhagat, J. V. Singh, A. Singh, A. Kumar, P. M. S. Bedi and H. Singh, *Bioorg. Chem.*, 2022, **118**, 105479.
12 R. D. Goff and J. S. Thorson, *Org. Lett.*, 2009, **11**, 461–464.
13 D. K. Sharma, B. Rah, M. R. Lambu, A. Hussain, S. K. Yousuf, A. K. Tripathi, B. Singh, G. Jamwal, Z. Ahmed and N. Chanauria, *MedChemComm*, 2012, **3**, 1082–1091.
14 B. Goel, N. Tripathi, D. Mukherjee and S. K. Jain, *Eur. J. Med. Chem.*, 2021, **213**, 113156.
15 M. A. Cinelli, *Med. Res. Rev.*, 2019, **39**, 1294–1337.
16 C. Reily, T. J. Stewart, M. B. Renfrow and J. Novak, *Nat. Rev. Nephrol.*, 2019, **15**, 346–366.
17 S. Wang, Q. He, J. Ye, Z. Kang, Q. Zheng, S. Liu, J. He and L. Sun, *Health Sci. J.*, 2020, **14**, 743.
18 K. Jain, P. Kesharwani, U. Gupta and N. K. Jain, *Biomaterials*, 2012, **33**, 4166–4186.
19 D. Shental-Bechor and Y. Levy, *Curr. Opin. Struct. Biol.*, 2009, **19**, 524–533.
20 J. M. Langenhan, N. R. Peters, I. A. Guzei, F. M. Hoffmann and J. S. Thorson, *Proc. Natl. Acad. Sci. U. S. A.*, 2005, **102**, 12305–12310.
21 D.-d. Wang, Y.-z. Bao, J. Liu, X.-k. Zhang, X.-s. Yao, X.-L. Sun and J.-S. Tang, *Bioorg. Med. Chem. Lett.*, 2017, **27**, 3359–3364.
22 B. R. Griffith, C. Krepel, X. Fu, S. Blanchard, A. Ahmed, C. E. Edmiston and J. S. Thorson, *J. Am. Chem. Soc.*, 2007, **129**, 8150–8155.
23 K. Singh, K. P. Singh, A. Equbal, S. S. Suman, A. Zaidi, G. Garg, K. Pandey, P. Das and V. Ali, *Biochimie*, 2016, **131**, 29–44.
24 J. Lam, M. Herant, M. Dembo and V. Heinrich, *Biophys. J.*, 2009, **96**, 248–254.
25 B. Gopu, P. Kour, R. Pandian and K. Singh, *Int. Immunopharmacol.*, 2023, **114**, 109591.
26 A. Das, M. C. Das, N. Das and S. Bhattacharjee, *Pharm. Biol.*, 2017, **55**, 998–1009.
27 P. C. Naha, M. Davoren, F. M. Lyng and H. J. Byrne, *Toxicol. Appl. Pharmacol.*, 2010, **246**, 91–99.
28 H. Lee, K.-H. Baek, T.-N. Phan, I. S. Park, S. Lee, J. Kim and J. H. No, *Biochem. Biophys. Res. Commun.*, 2021, **569**, 193–198.
29 A. Diotallevi, L. Scalvini, G. Buffi, Y. Pérez-Pertejo, M. De Santi, M. Verboni, G. Favi, M. Magnani, A. Lodola and S. Lucarini, *ACS Omega*, 2021, **6**, 35699–35710.
30 A. Roy, B. B. Das, A. Ganguly, S. Bose Dasgupta, N. V. Khalkho, C. Pal, S. Dey, V. S. Giri, P. Jaisankar and S. Dey, *Biochem. J.*, 2008, **409**, 611–622.
31 E. van den Bogaart, G. J. Schoone, P. England, D. Faber, K. M. Orrling, J.-C. Dujardin, S. Sundar, H. D. Schallig and E. R. Adams, *Antimicrob. Agents Chemother.*, 2014, **58**, 527–535.
32 J. Singh, M. I. Khan, S. P. S. Yadav, A. Srivastava, K. K. Sinha, P. Das and B. Kundu, *Int. J. Parasitol. Drugs Drug Resist.*, 2017, **7**, 337–349.
33 S. R. Chowdhury and H. K. Majumder, *Trends Biochem. Sci.*, 2019, **44**, 415–432.
34 J. A. Ibarra-Hernández, R. Gómez-Balderas, D. Nivón-Ramírez, J. G. García-Estrada, D. A. Mendoza-Jiménez, A. Martínez-Zaldívar, T. A. Cruz-Sánchez, N. Tovar-Betancourt,

R. A. Luna-Mora and J. G. Penieres-Carrillo, *J. Mol. Struct.*, 2022, **1249**, 131499.
35 P. Lei, M. Abdelrahim, S. D. Cho, S. Liu, S. Chintharlapalli and S. Safe, *Carcinogenesis*, 2008, **29**, 1139–1147.
36 A. Roy, S. Chowdhury, S. Sengupta, M. Mandal, P. Jaisankar, I. D'Annessa, A. Desideri and H. K. Majumder, *PLoS One*, 2011, **6**, e28493.
37 M. Garg and N. K. Jain, *J. Drug Targeting*, 2006, **14**, 1–11.
38 M. Garg, T. Dutta and N. K. Jain, *Eur. J. Pharm. Biopharm.*, 2007, **67**, 76–85.
39 Y. Oda, H. Yanagisawa, M. Maruyama, K. Hattori and T. Yamanoi, *Bioorg. Med. Chem.*, 2008, **16**, 8830–8840.
40 P. Pukanud, P. Peungvicha and N. Sarisuta, *Drug Delivery*, 2009, **16**, 289–294.